Immunity
Article

Intestinal Bacteria Trigger T Cell-Independent Immunoglobulin A_2 Class Switching by Inducing Epithelial-Cell Secretion of the Cytokine APRIL

Bing He,[1] Weifeng Xu,[1] Paul A. Santini,[1,3] Alexandros D. Polydorides,[1] April Chiu,[1] Jeannelyn Estrella,[1] Meimei Shan,[2] Amy Chadburn,[1] Vincenzo Villanacci,[4] Alessandro Plebani,[5] Daniel M. Knowles,[1] Maria Rescigno,[6] and Andrea Cerutti[1,3,*]
[1] Department of Pathology and Laboratory Medicine
[2] Department of Immunology and Microbiology
Weill Medical College of Cornell University, 1300 York Avenue, New York, NY 10021, USA
[3] Weill Graduate School of Medical Sciences of Cornell University, 1300 York Avenue, New York, NY 10021, USA
[4] Secondo Servizio di Anatomia Patologica, Spedali Civili di Brescia, P.le Spedali Civili 1, Brescia 25123, Italy
[5] Clinica Pediatrica e Istituto di Medicina Molecolare "A. Nocivelli," Universita' di Brescia, P.le Spedali Civili 1, Brescia 25123, Italy
[6] European Institute of Oncology (IEO), Via Ripamonti 435, Milano 20141, Italy
*Correspondence: acerutti@med.cornell.edu
DOI 10.1016/j.immuni.2007.04.014

SUMMARY

Bacteria colonize the intestine shortly after birth and thereafter exert several beneficial functions, including induction of protective immunoglobulin A (IgA) antibodies. The distal intestine contains IgA_2, which is more resistant to bacterial proteases than is IgA_1. The mechanism by which B cells switch from IgM to IgA_2 remains unknown. We found that human intestinal epithelial cells (IECs) triggered IgA_2 class switching in B cells, including IgA_1-expressing B cells arriving from mucosal follicles, through a $CD4^+$ T cell-independent pathway involving a proliferation-inducing ligand (APRIL). IECs released APRIL after sensing bacteria through Toll-like receptors (TLRs) and further increased APRIL production by activating dendritic cells via thymic stromal lymphopoietin. Our data indicate that bacteria elicit IgA_2 class switching by linking lamina propria B cells with IECs through a TLR-inducible signaling program requiring APRIL. Thus, mucosal vaccines should activate IECs to induce more effective IgA_2 responses.

INTRODUCTION

Antibody diversity is essential for protective immunity. Immature B cells generate antigen recognition diversity by assembling the antigen-binding variable region of immunoglobulins (Igs) from individual variable (V), diversity (D), and/or joining (J) gene segments through recombination-activating gene proteins (Schlissel, 2003). Mature B cells further diversify the antibody repertoire through V(D)J gene somatic hypermutation (SHM) and heavy-chain (H) class switch DNA recombination (CSR), two processes that require activation-induced cytidine deaminase (AID) (Honjo et al., 2002). While SHM introduces point mutations in the V(D)J exon, thereby providing the structural correlate for selection by antigen of higher-affinity mutants (Odegard and Schatz, 2006), CSR modulates the antibody effector functions by substituting IgM and IgD with IgG, IgA, or IgE (Chaudhuri and Alt, 2004).

IgA class switching enables antibody secretion onto mucosal surfaces (Brandtzaeg et al., 2001). In addition to targeting dietary antigens, toxins, and pathogenic microorganisms, IgA controls the growth of commensal bacteria and prevents their adhesion to intestinal epithelial cells (IECs) (Fagarasan et al., 2002; Macpherson and Uhr, 2004; Mestecky et al., 1999). Although coated with IgA, commensal bacteria survive and exert several beneficial functions, including synthesis of essential vitamins and protection against pathogens (Nagler-Anderson, 2001). In addition, commensal bacteria induce mucosal IgA class switching through a mechanism that remains poorly understood (Macpherson, 2006).

In general, IgA class switching requires the stimulation of B cells by $CD4^+$ T cells through CD40 ligand (CD40L) and cytokines, including interleukin (IL)-4, IL-10, and transforming growth factor (TGF)-β (Coffman et al., 1989; Fayette et al., 1997; Stavnezer, 1996). These signals induce AID expression and subsequent IgA CSR in B cells within the germinal center (GC) of mucosal inductive sites, including Peyer's patches (PPs) (Fagarasan and Honjo, 2003). Then, class-switched B cells differentiate into IgA-secreting plasmacytoid B cells, which migrate to the intestinal lamina propria (LP) under the influence of IEC-derived chemokines (Mora et al., 2006; Wilson and Butcher, 2004). Ultimately, IgA released at mucosal effector sites binds to a polymeric Ig receptor (pIgR) on the basolateral surface of IECs and translocates onto the mucosal surface to exert its protective function (Brandtzaeg et al., 2001).

IECs further promote mucosal immunity by cross talking with dendritic cells (DCs) (Neutra et al., 2001). While

sampling antigen in the intestinal lumen (Rescigno et al., 2001), DCs receive signals from thymic stroma lymphopoietin (TSLP), an IL-7-like cytokine released by IECs (Ziegler and Liu, 2006). In addition to secreting plasma cell-inducing IL-6 (Sato et al., 2003), TSLP-conditioned DCs prime $CD4^+$ T helper (Th) cells to undergo type-2 (Th2) differentiation and IL-4 and IL-10 secretion (Rimoldi et al., 2005). Together with TGF-β, these mediators enable mucosal B cells to skew their antibody repertoire toward IgA (Coffman et al., 1989; Fagarasan and Honjo, 2003).

In addition to initiating T cell-dependent (TD) IgA responses to pathogens, DCs trigger T cell-independent (TI) IgA responses to commensals. In mice, this TI pathway involves activation of broadly reactive $CD5^+$ B-1 cells in the intestinal LP by commensal-loaded DCs (Fagarasan et al., 2001; Macpherson and Uhr, 2004; Mora et al., 2006). Humans lack canonical B-1 cells but undergo TI IgA CSR in response to DCs expressing B cell-activation factor of the tumor necrosis factor family (BAFF) and a proliferation-inducing ligand (APRIL) (Litinskiy et al., 2002). These CD40L-related molecules are also produced by mucosal epithelial cells and may account for IgA production in children with defective CD40L signaling (Jain et al., 2004; Kato et al., 2006; Xu et al., 2007). Accordingly, defects of BAFF and APRIL signaling cause IgA deficiency (Castigli et al., 2004, 2005; Salzer et al., 2005).

Human B cells produce two IgA subclasses (Stavnezer, 1996). Whereas systemic B cells produce mostly IgA_1, mucosal B cells produce both IgA_1 and IgA_2. The latter is very abundant in the distal intestine and is more resistant than IgA_1 to degradation by bacterial proteases (Mestecky et al., 1999). The regulation of IgA_2 CSR remains elusive. We hypothesized that intestinal IgA_2 production occurs in a TI fashion because IgA_2 can be induced by DCs (Fayette et al., 1997) and, similar to B-1-derived IgA (Fagarasan and Honjo, 2003), can recognize multiple bacterial products (Lue et al., 1988; Tarkowski et al., 1990).

We found that APRIL was essential to trigger IgA_2 class switching in human B cells, including IgA_1-producing effector B cells. IECs released APRIL after sensing bacteria through Toll-like receptors (TLRs) and further augmented APRIL production by stimulating DCs through TSLP. Our data suggest that intestinal bacteria induce IgA_2 diversification of LP B cells arriving from mucosal lymphoid follicles by linking them with IECs via a TI signaling program involving APRIL.

RESULTS

IgA_2-Producing B Cells Are Abundant in the Intestinal LP

IgA_2 production occurs mainly in the lower intestinal tract and positively correlates with the heavier bacterial load of this mucosal district (Crago et al., 1984; Kett et al., 1986; Mestecky et al., 1999). Thus, we wondered whether IgA_2-expressing B cells are more abundant near the bacteria-colonized lumen of the colon. To address this question, we took advantage of an immunofluorescence-based approach to determine the presence of IgA_1 and IgA_2 in human colon tissue samples. We found that the LP contained more IgA_2^+ B cells than IgA_1^+ B cells (Figures 1A and 1B; Figure S1 in the Supplemental Data available online). Similarly, IECs contained more IgA_2 than IgA_1. In contrast, PP B cells expressed more IgA_1 than IgA_2 (Figures 1C and 1D). Some of these PP IgA_1^+ B cells had a GC phenotype as they expressed AID, a B cell-restricted protein associated with ongoing CSR (Fagarasan et al., 2002), in addition to B cell-specific activation protein (BSAP), a nuclear transcription factor essential for Ig gene transcription (Stavnezer, 1996). In general, LP and PPs from the colon included more IgA_2^+ B cells than LP and PPs from the jejunum (Figure 1E). These intestinal districts contained more IgA_2^+ B cells than the aerodigestive mucosa of palatine tonsils and nonmucosal districts, such as peripheral blood (PB), spleen, and systemic lymph nodes. Thus, our data indicate that the LP of the distal gut provides a niche favorable for IgA_2 production.

IgA_2 CSR Requires APRIL

Human B cells undergo IgA CSR in response to CD40L, BAFF, or APRIL and IL-10 (Fayette et al., 1997; Litinskiy et al., 2002; Xu et al., 2007). The requirements for IgA_2 CSR remain elusive. To elucidate these requirements, we purified preswitched IgD^+ B cells and cultured them with various IgA-inducing stimuli. Then, we determined the induction of IgA_1 and IgA_2 CSR byproducts at appropriate time points through standard techniques. Purified IgD^+ B cells upregulated surface IgA_1 upon exposure to IL-10 together with BAFF, APRIL, or CD40L, the last being more efficient than BAFF or APRIL (Figure 1F; Figure S2A). Upregulation of surface IgA_1 was associated with induction of postswitch I_μ-$C_\alpha 1$ transcripts, a hallmark of IgA_1 CSR (Figures S2B and S2C). In addition to IgA_1, APRIL and, to a lesser extent, BAFF induced surface IgA_2 as well as postswitch I_μ-$C_\alpha 2$ transcripts (Figure 1F; Figures S2B and S2C), a hallmark of IgA_2 CSR. Although capable of delivering powerful survival and proliferation signals, CD40L did not induce surface IgA_2 and postswitch I_μ-$C_\alpha 2$ transcripts. Induction of IgA_1 and IgA_2 secretion required an additional signal from surface Ig, at least in B cells exposed to BAFF or APRIL. Of note, some APRIL-induced IgA_2 reacted against commensals, such as *Lactobacillus plantarum*, LPS, and flagellin (Figure S3A). Although it had poor IgA_2-inducing activity, BAFF enhanced APRIL-induced IgA_2 secretion (Figure S3B), perhaps by augmenting IgA_2^+ B cell survival (Schneider, 2005). These data indicate that APRIL is essential to initiate IgA_2 CSR.

IECs Express APRIL

Having shown that APRIL is required for IgA_2 production, we wished to identify the source of APRIL in the gut. To address this point, we performed APRIL-specific immunofluorescence on human colon tissue samples and Caco-2, a human colon IEC line that recapitulates most of the properties of primary IECs, including the ability to form a polarized epithelial monolayer with tight junctions (Rescigno et al., 2001; Rimoldi et al., 2005). We found

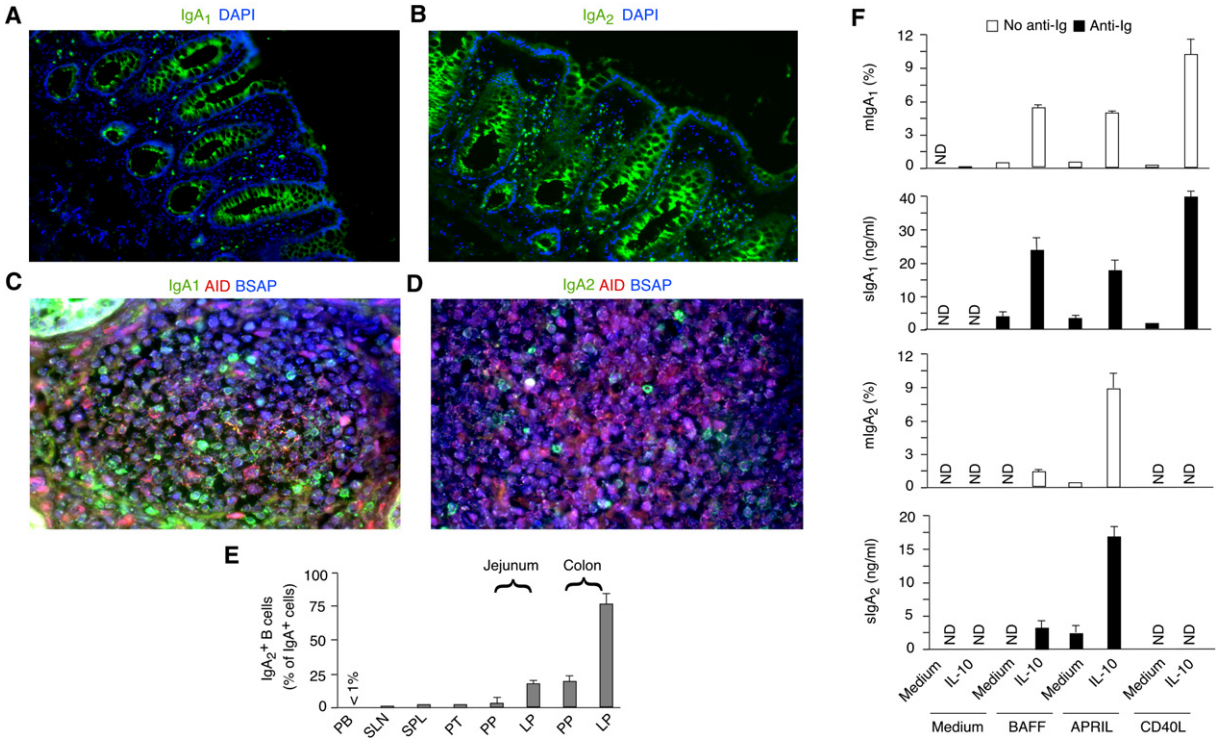

Figure 1. IgA$_2$ Production Is More Abundant in the Intestinal LP and Requires APRIL

(A and B) Immunofluorescence analysis of human colon mucosa stained for IgA$_1$ or IgA$_2$ (green). DAPI (blue) counterstains nuclei. Original magnification, ×5.

(C and D) Colon PPs stained for IgA$_1$ or IgA$_2$ (green), AID (red), and BSAP (blue). Original magnification, ×10.

(E) Percentage of IgA$_2^+$ B cells in PB, systemic lymph nodes (SLNs), spleen (SPL), palatine tonsil (PT), and PPs and LP from proximal (jejunum) or distal (colon) intestine. Percentages were calculated from 200 IgA$^+$ cells within tissue sections from three different donors double-stained for IgA and IgA$_2$.

(F) Flow cytometric analysis of membrane IgA$_1$ (mIgA$_1$) and mIgA$_2$ and ELISA of secreted IgA$_1$ (sIgA$_1$) and sIgA$_2$ from PB IgD$^+$ B cells cultured for 4 or 8 days with or without BAFF, APRIL, or CD40L in the presence or absence of IL-10. sIgA production was optimized with an antibody to the μ chain of Igs (anti-Ig) (solid bars).

Shown in (A)–(D) are 1 of 5 experiments yielding similar results, and (E) and (F) summarize 3 experiments (bars indicate mean SD).

abundant APRIL in IECs lining the distal intestinal mucosa (Figures 2A and 2B; Figure S4B) and in Caco-2 IECs (Figure 2C). We also detected APRIL in dendritic and plasmacytoid cells in the LP (Figure 2D) but not in PPs (not shown). In addition to APRIL, IECs expressed BAFF (Figure S3D), an APRIL-related protein that we had previously shown to possess IgA$_1$ and, to some extent, IgA$_2$ class switch-inducing activity. These findings indicate that IECs constitute a major source of IgA-inducing factors in the digestive tract.

IECs Release APRIL after Sensing Bacteria through TLRs

IECs may produce abundant APRIL because of their genetic makeup. Accordingly, IECs contained more APRIL-encoding *TNFSF13* transcripts than epithelial cells from epidermis, lung, cervix, uterus, and mouth (Figure 2E). APRIL production by IECs may also stem from interaction with bacteria. Indeed, Caco-2 IECs upregulated the synthesis of *TNFSF13* transcripts (Figure 2F) and the release of APRIL (Figure 2G) upon exposure to noninvasive commensal bacteria, such as *Lactobacillus plantarum* and *Bacillus subtilis*, or invasive pathogenic bacteria, such as the *aroA* strain of *Salmonella typhimurium*. A noninvasive *aroA-invA* mutant of *Salmonella typhimurium* lacking the pathogenicity island 1-associated *invA* gene retained APRIL-inducing activity on IECs. Of bacterial TLR ligands (Takeda et al., 2003), LPS (a cell-wall component that binds TLR4) and flagellin (a flagellum-associated protein that binds TLR5) augmented APRIL production by Caco-2 IECs, whereas peptidoglycan (PGN) (a bacterial-wall component that binds TLR1, TLR2, and TLR6), cytidylate-phosphate-guanylate oligodeoxynucleotide (CpG ODN) (a bacterial DNA analog that binds TLR9), and poly inosinic cytidylic acid (I:C) (a viral RNA analog that binds TLR3), did not. Yet, PGN augmented APRIL production by flagellin-activated Caco-2 IECs (Figure S4A). Furthermore, CpG ODN, PGN, and poly(I:C) had APRIL-inducing activity on HT-29 IECs in addition to LPS and flagellin (Figure S4B). Caco-2 IECs lacking MyD88, a key TLR signaling protein, released no or little APRIL in response to flagellin (Figure 2H) or bacteria (not shown). Thus, induction of APRIL by bacteria requires TLR signaling in IECs, but not invasion of IECs.

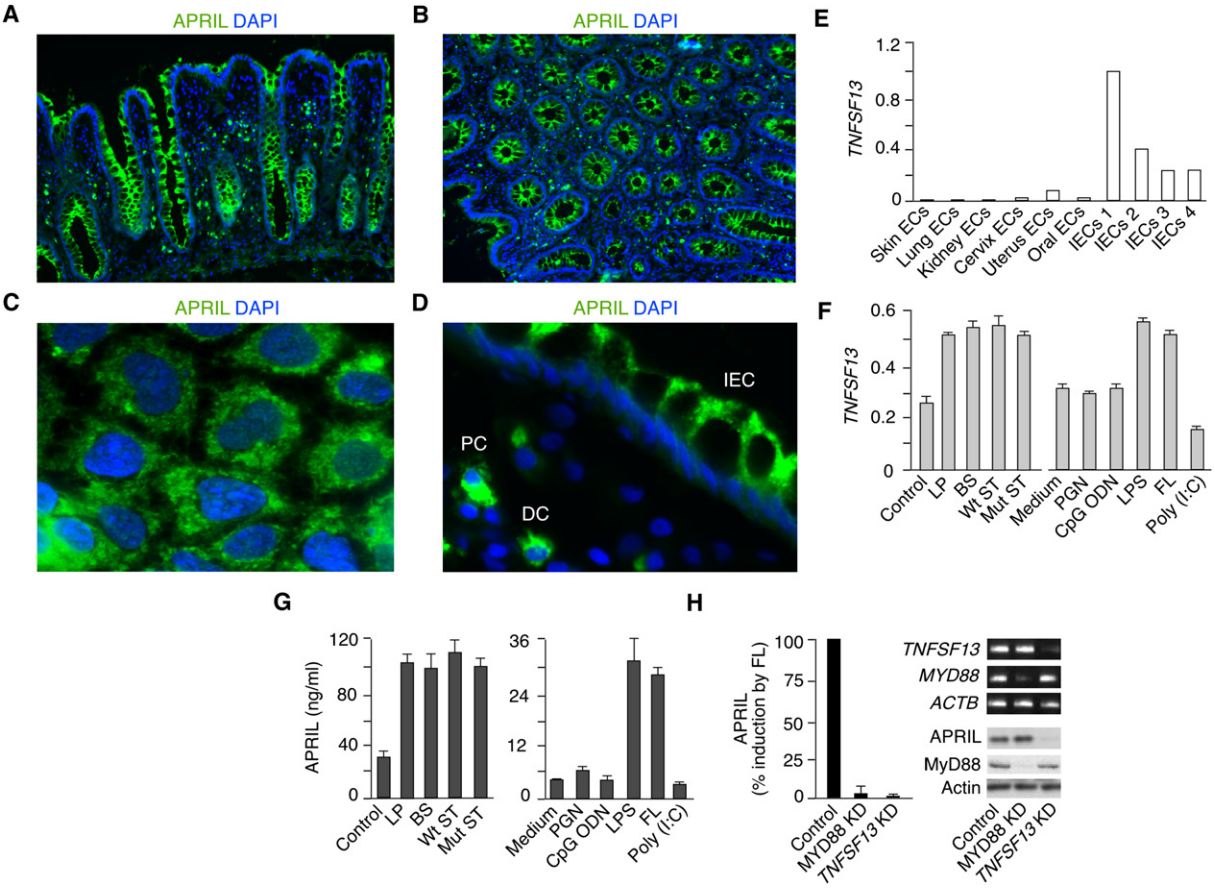

Figure 2. IECs Release APRIL after Sensing Bacteria through a TLR-Dependent Pathway

(A–D) Immunofluorescence analysis of intestinal mucosa (A, B, and D) and Caco-2 IECs (C) stained for APRIL (green) and DAPI (blue). PC indicates a cell with plasmacytoid morphology. Original magnification, ×5 (A and B), ×63 (C), and ×40 (D).

(E) Real-time RT-PCR of APRIL-encoding *TNFSF13* transcripts from HT-29 (1), Caco-2 (2), T84 (3), and HCA7 (4) IEC lines, primary epidermal and oral epithelial cells, and lung A549, uterine RL95-2, kidney 293, and cervical HeLa epithelial-cell lines. *TNFSF13* mRNA was normalized to *ACTB* mRNA.

(F) *TNFSF13* from Caco-2 IECs incubated with control medium, *Lactobacillus plantarum* (LP), *Bacillus subtilis* (BS), wild-type (WT) invasive *aroA* strain of *Salmonella typhimurium* (ST), mutant (Mut) noninvasive *aroA-InvA* strain of ST lacking the *invA* gene, medium alone, PGN, CpG ODN, LPS, flagellin (FL), or poly(I:C) for 2 days. Bacteria and bacterial products were added from the apical surface of IECs.

(G) ELISA of APRIL released by Caco-2 IECs cultured as in (F).

(H) ELISA of APRIL released by control, MYD88 KD, and *TNFSF13* KD Caco-2 IECs exposed to flagellin (FL) for 2 days. Control refers to IECs nucleofected with an irrelevant siRNA. Results are expressed as percentage of released APRIL compared to IECs exposed to no siRNA. Upper three panels on the right show RT-PCRs of *TNFSF13*, MYD88, and *ACTB* transcripts from IECs treated with various siRNAs. Bottom three panels on the right show immunoblots of APRIL, MyD88, and actin proteins from IECs treated with various siRNAs.

Shown in (A)–(E) are 1 of 3 experiments yielding similar results, and (F)–(H) summarize 3 experiments (bars indicate mean SD).

APRIL Cooperates with Bacterial Products to Induce IgA$_2$ CSR

Knowing that some TLRs signal CSR in B cells (He et al., 2004), we wondered whether APRIL and TLR ligands cooperate to induce IgA$_2$ CSR. Of APRIL-inducing TLR ligands, flagellin can be expressed by commensal bacteria and activates DCs and B cells in addition to IECs (Abreu et al., 2005; Takeda et al., 2003). Accordingly, we detected the flagellin receptor TLR5 not only in IECs, but also in LP DCs and PP B cells (Figures 3A–3C). In the presence of APRIL or FL, IgD$^+$ B cells upregulated germline I_α2-C_α2 and *AICDA* transcripts (Figures 3D and 3E), two IgA$_2$ CSR-associated products. A combination of APRIL and flagellin not only further increased I_α2-C_α2 and *AICDA* expression, but also induced switch I_α-C_μ circular transcripts, a hallmark of IgA CSR (Fagarasan et al., 2001; Litinskiy et al., 2002), as well as IgA$_2$ secretion (Figures 3F and 3G). CpG ODN had enhancing effects similar to those of flagellin (not shown), indicating that bacterial products cooperate with APRIL to induce IgA$_2$ CSR in IgD$^+$ B cells.

IECs Induce IgA$_2$ CSR by Producing APRIL in Response to Bacterial Products

By showing that FL stimulates IECs to release APRIL and cooperates with APRIL to induce IgA$_2$ CSR, our data

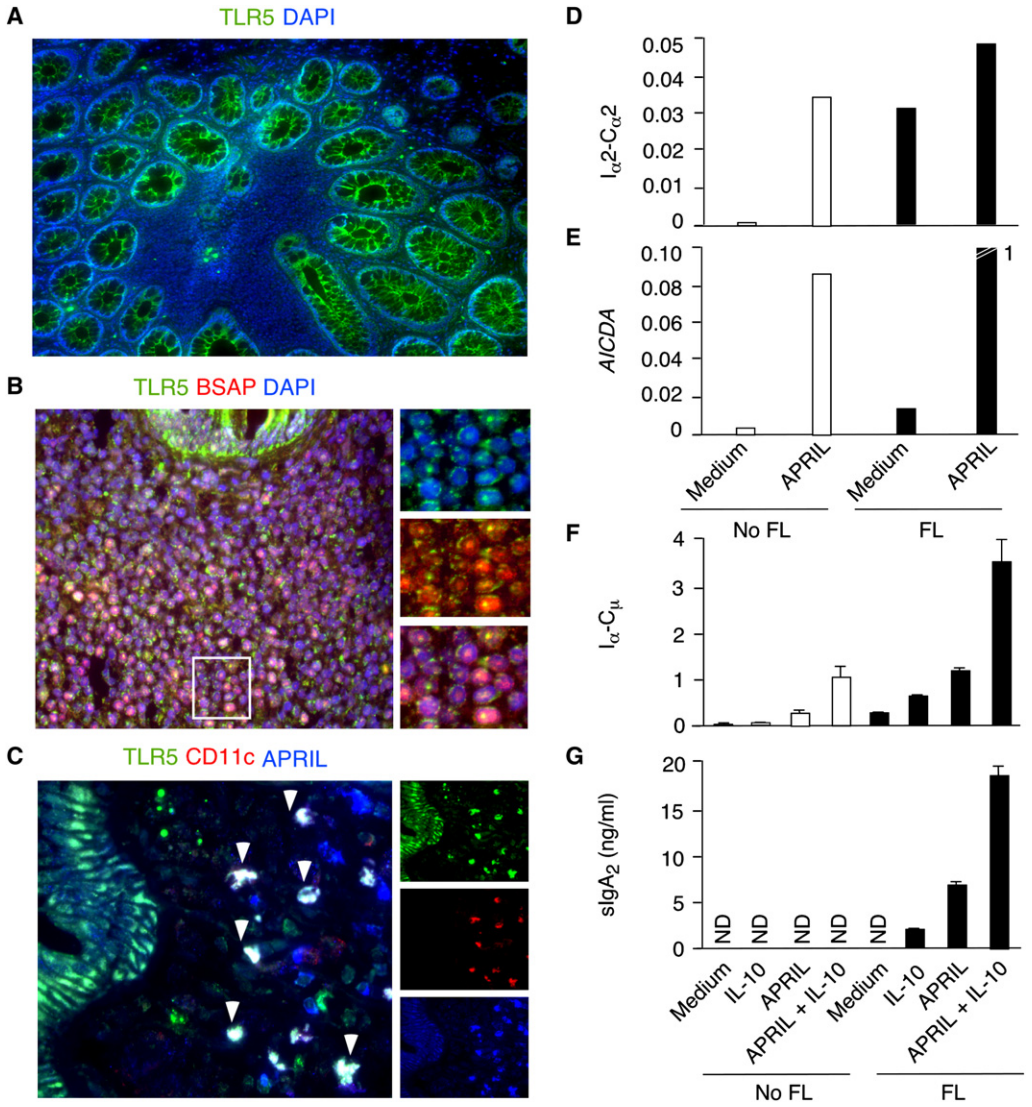

Figure 3. APRIL Collaborates with Flagellin to Induce IgA$_2$ CSR

(A–C) Immunofluorescence analysis of intestinal mucosa stained for TLR5 (green), BSAP or CD11c (red), and DAPI or APRIL (blue). In (B), bottom open box in left image corresponds to magnified TLR5$^+$BSAP$^+$ Peyer's patch B cells in rightmost images. In (C), arrowheads point to LP DCs coexpressing TLR5, CD11c, and APRIL. Original magnification, ×10 (A and B) and ×40 (C).

(D–F) Real-time RT-PCR of $I_\alpha 2$-$C_\alpha 2$, *AICDA*, and I_α-C_μ transcripts from PB IgD$^+$ B cells incubated in the presence or absence of APRIL and/or flagellin (FL) for 2 days. $I_\alpha 2$-$C_\alpha 2$ and *TNFSF13* mRNAs were normalized to *ACTB* mRNA, whereas I_α-C_μ mRNA was normalized to I_μ-C_μ mRNA.

(G) Flow cytometric analysis of mIgA$_2$ and ELISA of sIgA$_2$ from PB IgD$^+$ B cells cultured for 4 and 8 days, respectively, with or without IL-10 and/or APRIL in the presence or absence of flagellin (FL).

Shown in (A)–(E) are 1 of 3 experiments yielding similar results, and (F) and (G) summarize 3 experiments (bars indicate mean SD).

suggest that mucosal IgA$_2$ production involves a crosstalk between IECs and B cells. The cooperation between IECs and B cells was further investigated in a simplified in vitro model of intestinal mucosa consisting of IECs and B cells spatially distributed in a manner similar to that observed in vivo. Caco-2 IECs were seeded on the upper chamber of a transwell system to form a polarized monolayer (Rescigno et al., 2001), whereas preswitched IgD$^+$ B cells were placed in the lower chamber (Figure S4C). Bacteria and bacterial products were added from the apical surface of IECs. To compensate for the lack of DCs producing IL-10, the lower chamber was supplemented with IL-10. In the presence of flagellin, IECs induced IgD$^+$ B cells to upregulate $I_\alpha 2$-$C_\alpha 2$ and *AICDA* expression and undergo IgA$_2$ secretion (Figures 4A–4C). This induction required expression of MyD88 and APRIL, but not BAFF by IECs (Figure 4D). LPS and *Lactobacillus plantarum* had a comparable IgA$_2$-inducing effect (Figures S5A–S5C). Flagellin also induced $I_\alpha 1$-$C_\alpha 1$ and some IgA$_1$ through MyD88 and both BAFF and APRIL (Figures S6A–S6C). Of note, IEC-induced IgA$_1$ was less than IgA$_2$, suggesting that some IEC-induced IgA$_1^+$ B cells undergo sequential IgA$_2$ class

switching. These data indicate that IECs induce IgA_2 CSR via APRIL after sensing bacteria through TLRs.

Intestinal LP B Cells Actively Undergo IgA CSR In Situ

Having shown that IECs induce IgA_2 CSR in vitro, we wondered whether LP B cells undergo IgA_2 CSR in vivo. Ongoing CSR is associated with expression of AID (Fagarasan et al., 2001). We identified *AICDA* transcripts and AID protein in LP B cells, including IgA_1^+ B cells lodged in the proximity of or within the intestinal epithelium (Figures 4E and 4F; Figure S7A). AID, IgA_2, and APRIL had similar expression patterns in both intestinal and aerodigestive mucosae (Figures S7B and S8A–S8C). AID was also detected in IgD^+ and a few IgG^+ LP B cells (Figure 4G). In addition to *AICDA* transcripts, ex vivo isolated LP B cells contained excised switch α (S_α)-S_μ switch circles (Figure 5A; Figures S7C), a hallmark of ongoing IgM-to-IgA CSR. Because of the high degree of sequence identity between $S_\alpha1$ and $S_\alpha2$ regions, we could not distinguish $S_\alpha1$-S_μ from $S_\alpha2$-S_μ switch circles, nor could we detect $S_\alpha2$-$S_\alpha1$ switch circles originating from IgA_1-to-IgA_2 CSR. Some LP $IgA_1^+AID^+$ B cells expressed not only AID and BSAP, as actively class-switching GC B cells do, but also B-lymphocyte activation-induced maturation protein 1 (Blimp-1) and CD138 (Figure 5B), as plasma cells do (Calame, 2001). LP $IgA_1^+AID^+$ B cells also expressed interferon regulatory factor 4 (IRF4), a CSR-inducing transcription factor associated with GC, extrafollicular, and plasmacytoid B cells (Cattoretti et al., 2006; He et al., 2004; Klein et al., 2006). These data show that the human LP is a site of active IgA CSR and suggest that LP IgA_1^+ effector B cells arriving from mucosal GCs undergo IgA_2 CSR in situ.

Intestinal LP B Cells Undergo IgA_2 CSR in a T Cell- and CD40-Independent Fashion

To elucidate the nature of CSR events in LP IgA_2^+ B cells, we analyzed the composition of their chromosomal S-S DNA junctions. LP IgA_2^+ B cells contained chromosomal S_μ-$S_\alpha2$, S_μ-$S_\alpha1$-$S_\alpha2$ and, less frequently, S_μ-$S_\gamma1$-$S_\alpha2$ junctions originating from direct or sequential IgA_2 CSR events (Figure 5C; Figures S9A). Similar S-S junctions were detected in tonsillar IgA_2^+ B cells (Figures S9B and S9C). In additional experiments, we took advantage of mucosal specimens from a patient with CD40 deficiency resulting from congenital type-3 hyper-IgM syndrome (HIGM3) and a patient with $CD4^+$ T cell deficiency resulting from acquired immunodeficiency syndrome (AIDS) to verify whether IgA_2 CSR requires help from $CD4^+$ T cells in vivo (Ferrari et al., 2001; Hel et al., 2006). The intestinal LP from both HIGM3 and AIDS patients showed conserved expression of IgA_1, IgA_2, AID, *AICDA*, and APRIL (Figures 6A and 6B; Figures S10A–S10C). Considering that CD40 deficiency results in a lack of systemic and mucosal GCs (Castigli et al., 1994; Ferrari et al., 2001), these data confirm that LP B cells can undergo IgA_2 CSR in situ through a TI- and CD40-independent mechanism involving APRIL.

APRIL Induces Sequential IgA_2 CSR in IgA_1^+ or IgG_1^+ B Cells

Having detected chromosomal S_μ-$S_\alpha1$-$S_\alpha2$ and S_μ-$S_\gamma1$-$S_\alpha2$ junctions in LP B cells, we wondered whether IgA_1^+ or IgG_1^+ B cells undergo sequential IgA_2 CSR in response to APRIL. In the presence of IL-10, APRIL augmented chromosomal DNA recombination to $S_\alpha2$ in IgG_1^+ or IgA_1^+ B cells (Figure 6C; Figures S11A and S11B). This effect was associated with induction of germline $I_\alpha2$-$C_\alpha2$, *AICDA* and postswitch I_μ-$C_\alpha2$ transcripts as well as membrane and secreted IgA_2 proteins (Figures 6D and 6E; Figure S11C). CD40L induced similar effects, although less than APRIL and only in IgG_1^+ B cells. Unlike APRIL, CD40L did not induce IgA_2 secretion. These data indicate that APRIL is required for IgA_1^+ and IgG_1^+ B cells to undergo sequential IgA_2 CSR as well as IgA_2 secretion.

IECs Stimulate APRIL Production by DCs through TSLP

In agreement with prior studies on in vitro generated myeloid DCs (Litinskiy et al., 2002), we detected APRIL in myeloid $CD11c^+$ DCs within the intestinal LP (Figure 7A). Some of these DCs were proximal to IgA_1^+ B cells, whereas others were intercalated between IECs and emanated projections into the intestinal lumen. Thus, we hypothesized that mucosal DCs express APRIL upon exposure to bacterial and epithelial products, including TSLP (Rescigno et al., 2001; Rimoldi et al., 2005). Consistent with this possibility, flagellin upregulated the expression of *TSLP* transcripts by Caco-2 IECs (Figures 7B and 7C). Furthermore, flagellin cooperated with TSLP to upregulate the expression of TSLP receptor-encoding cytokine receptor-like factor 2 (*CRFL2*) and *TNFSF13* transcripts as well as the release of APRIL and IL-10 by myeloid DCs (Figures 7D–7F). In the presence of flagellin, TSLP-sufficient Caco-2 IECs upregulated the expression of *TNFSF13*, APRIL, and IL-10 by myeloid DCs, whereas TSLP-deficient Caco-2 IECs did not (Figures 7G–7I). LPS, PGN, and *Lactobacillus plantarum* recapitulated the effects of flagellin on IECs and myeloid DCs (not shown). Thus, bacteria and IECs cooperatively induce APRIL in mucosal DCs through TSLP.

TSLP-Conditioned DCs Enhance IEC-Induced IgA_2 CSR through APRIL

Having shown that IECs increase APRIL production by myeloid DCs via TSLP, we verified whether DCs augment IEC-induced IgA_2 class switching. IECs were placed in the upper chamber of a transwell system, whereas DCs and IgD^+ B cells were placed in the lower chamber. In the presence of flagellin, DCs induced as much IgA_2 production as Caco-2 IECs (Figure 7J). IgA_2 production was further upregulated by TSLP, and this upregulation could be prevented by B cell maturation-antigen (BCMA)-Ig, a soluble APRIL decoy receptor that prevents activation of B cells by APRIL (Litinskiy et al., 2002). In the presence of flagellin, TSLP-sufficient IECs and DCs induced as much IgA_2 as DCs exposed to both flagellin and TSLP. Lack of TSLP in IECs or addition of BCMA-Ig abolished induction of

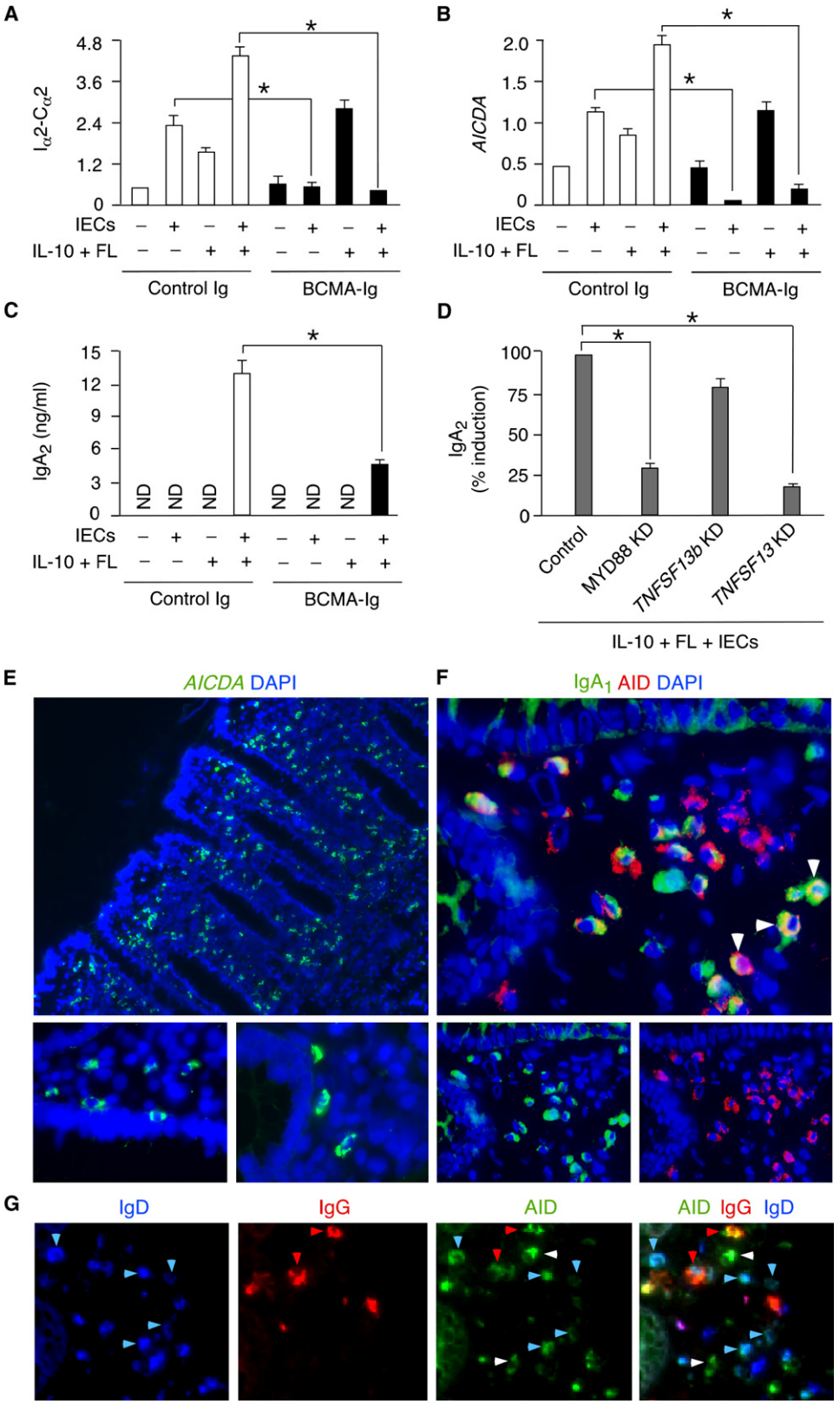
A
$I_\alpha 2$-$C_\alpha 2$
4.8
3.6
2.4
1.2
0
IECs
IL-10 + FL
Control Ig
BCMA-Ig
B
AICDA
2.0
1.5
1.0
0.5
0
C
IgA$_2$ (ng/ml)
15
12
9
6
3
0
ND
D
IgA$_2$ (% induction)
100
75
50
25
0
Control
MYD88 KD
TNFSF13b KD
TNFSF13 KD
IL-10 + FL + IECs
E
AICDA DAPI
F
IgA$_1$ AID DAPI
G
IgD
IgG
AID
AID IgG IgD

IgA_2 by IECs and DCs. Thus, in addition to directly inducing IgA_2 class switching through APRIL, bacteria-activated IECs enhance the APRIL-dependent IgA_2-inducing activity of myeloid DCs via TSLP (Figure S12).

DISCUSSION

We have reported here that APRIL is essential to trigger IgA_2 CSR in B cells, including IgA_1-expressing effector B cells arriving from mucosal lymphoid follicles. IECs released APRIL after sensing bacteria through TLRs and further augmented APRIL production by activating myeloid DCs via TSLP. Our data suggest that intestinal bacteria elicit IgA_2 class switching by linking LP B cells with IECs through a $CD4^+$ T cell- and CD40L-independent pathway involving APRIL.

The intestine is the largest lymphoid organ of our body, and every day intestinal plasma cells produce more antibodies than all other lymphoid organs combined, including spleen, lymph nodes, and bone marrow (Brandtzaeg et al., 2001; Mestecky et al., 1999). Although the remarkable dominance of IgA in the intestine has been known for decades, fine details of the mechanism underlying IgA class switching, mucosal homing of IgA-producing plasma cells, and transepithelial IgA transport continue to emerge with an impressive frequency (Mora et al., 2006). Nonetheless, many aspects of mucosal immunity remain unclear, and in particular scarce data are available on IgA_2. This IgA subclass is predominant in the lower human intestinal tract, is more resistant than IgA_1 to bacterial degradation, and is often reactive against highly conserved bacterial products, thus resembling polyreactive IgA antibodies released by mouse B-1 cells (Crago et al., 1984; Fagarasan and Honjo, 2003; Kett et al., 1986; Macpherson, 2006; Mestecky et al., 1999; Tarkowski et al., 1990). The present data indicate that, similar to mouse B-1 cells (Fagarasan et al., 2001), human IgA_2 B cell precursors undergo TI class switching in the intestinal LP.

One feature unique to mucosal surfaces is the crucial role of epithelial cells in the initiation and modulation of immune responses (Neutra et al., 2001; Xu et al., 2007). Functional interdependence of IECs and B cells has been amply documented and entails release of chemokines that promote recruitment of IgA-producing plasma cells to the intestinal LP (Wilson and Butcher, 2004), production of cytokines that enhance the terminal differentiation of arriving IgA-producing plasma cells (Mestecky et al., 1999), and transportation of IgA onto the mucosal surface through pIgR (Brandtzaeg et al., 2001). Our data indicate that IECs intersect humoral immunity by inducing IgA_2 CSR in LP B cells via APRIL.

We identified APRIL as an essential IgA_2 CSR-inducing factor. In agreement with recent studies showing production of APRIL and BAFF by epithelial cells from the respiratory tract (Kato et al., 2006; Xu et al., 2007), we found that IECs are a major source of APRIL in the gut. Production of APRIL by IECs is at least in part genetically determined as IECs expressed more APRIL-encoding *TNFSF13* transcripts than epithelial cells from nonintestinal districts. Commensal bacteria further enhance APRIL expression by activating IECs via TLRs. Thus, steady-state TLR signaling as induced by commensal bacteria could maintain intestinal homeostasis not only by promoting IEC growth and repair (Rakoff-Nahoum et al., 2004), but also by eliciting production of protective IgA_2 via APRIL. In addition to APRIL, IECs released BAFF, which not only triggered IgA_1 CSR, but also augmented APRIL-induced IgA_2 secretion, perhaps by delivering prosurvival signals to IgA_2-producing B cells.

Our findings suggest that bacteria-activated IECs utilize APRIL to generate IgA_2-inducing signals in LP B cells arriving from PPs, including effector IgA_1^+ B cells. Several lines of evidence support this model. First, the intestinal LP contained more IgA_2 and less IgA_1 than PPs. Second, some LP IgA_1^+ B cells expressed AID, a hallmark of ongoing CSR, along with phenotypic traits evocative of late GC B cells-early plasma cells. Third, LP IgA_2^+ plasmablasts harbored genomic $S_\alpha1$-$S_\alpha2$ DNA junctions originating from sequential IgA_2 CSR events. Fourth, APRIL, a key IEC-derived factor, elicited sequential IgA_2 CSR in purified IgA_1^+ B cells. Thus, effector IgA_1^+ B cells emerging from the GC of PPs may undergo APRIL-dependent sequential CSR as mechanism to acquire protease-resistant IgA_2, which is more suited than IgA_1 to cope with the dense commensal microflora of the distal intestine.

IgG^+ effector B cells may be also targeted by IEC-derived APRIL to undergo sequential IgG_1-to-IgA_2 CSR in the LP, because we could detect AID in LP IgG^+ B cells as well as genomic $S_\gamma1$-$S_\alpha2$ DNA junctions in LP IgA_2^+ plasmablasts. In addition, APRIL triggered IgA_2 CSR in purified IgG_1^+ B cells. Of note, $S_\gamma1$-$S_\alpha2$ junctions were less frequent than $S_\alpha1$-$S_\alpha2$ and S_μ-$S_\alpha2$ junctions, which

Figure 4. IECs Induce IgA_2 CSR by Releasing APRIL after Sensing Bacteria

(A and B) Real-time RT-PCR of $I_\alpha2$-$C_\alpha2$ and *AICDA* transcripts from PB IgD^+ B cells incubated with or without IECs, IL-10, and/or FL in the presence of control Ig or BCMA-Ig for 2 days. FL was added from the apical surface of IECs. $I_\alpha2$-$C_\alpha2$ and *AICDA* mRNAs were normalized to *ACTB* mRNA.

(C) ELISA of $sIgA_2$ from PB IgD^+ B cells cultured for 8 days as in (A). ND, not detected.

(D) $sIgA_2$ from PB IgD^+ B cells cultured for 8 days with control, MYD88 KD, and *TNFSF13* KD Caco-2 IECs and in the presence of FL and IL-10. Control refers to Caco-2 IECs nucleofected with an irrelevant siRNA. Results are expressed as percentage of released $sIgA_2$ compared to Caco-2 IECs exposed to no siRNA.

(E) In situ hybridization of *AICDA* (green). DAPI stains intestinal nuclei (blue). Bottom images show periepithelial *AICDA*$^+$ B cells. Original magnification, ×10 (top) and ×40 (bottom).

(F) Intestinal mucosa stained for IgA_1 (green), AID (red), and DAPI (blue). Arrowheads point to $IgA_1^+AID^+$ B cells. Original magnification, ×63.

(G) Intestinal mucosa stained for AID (green), IgG (red), and IgD (blue). Blue, red, and white arrowheads point to IgD^+ (blue), IgG_1^+, and double-negative B cells expressing AID, respectively. Original magnification, ×40.

Three experiments are summarized in (A)–(D) (bars indicate mean SD; *$p < 0.05$), and (E)–(G) show 1 of 3 experiments yielding similar results.

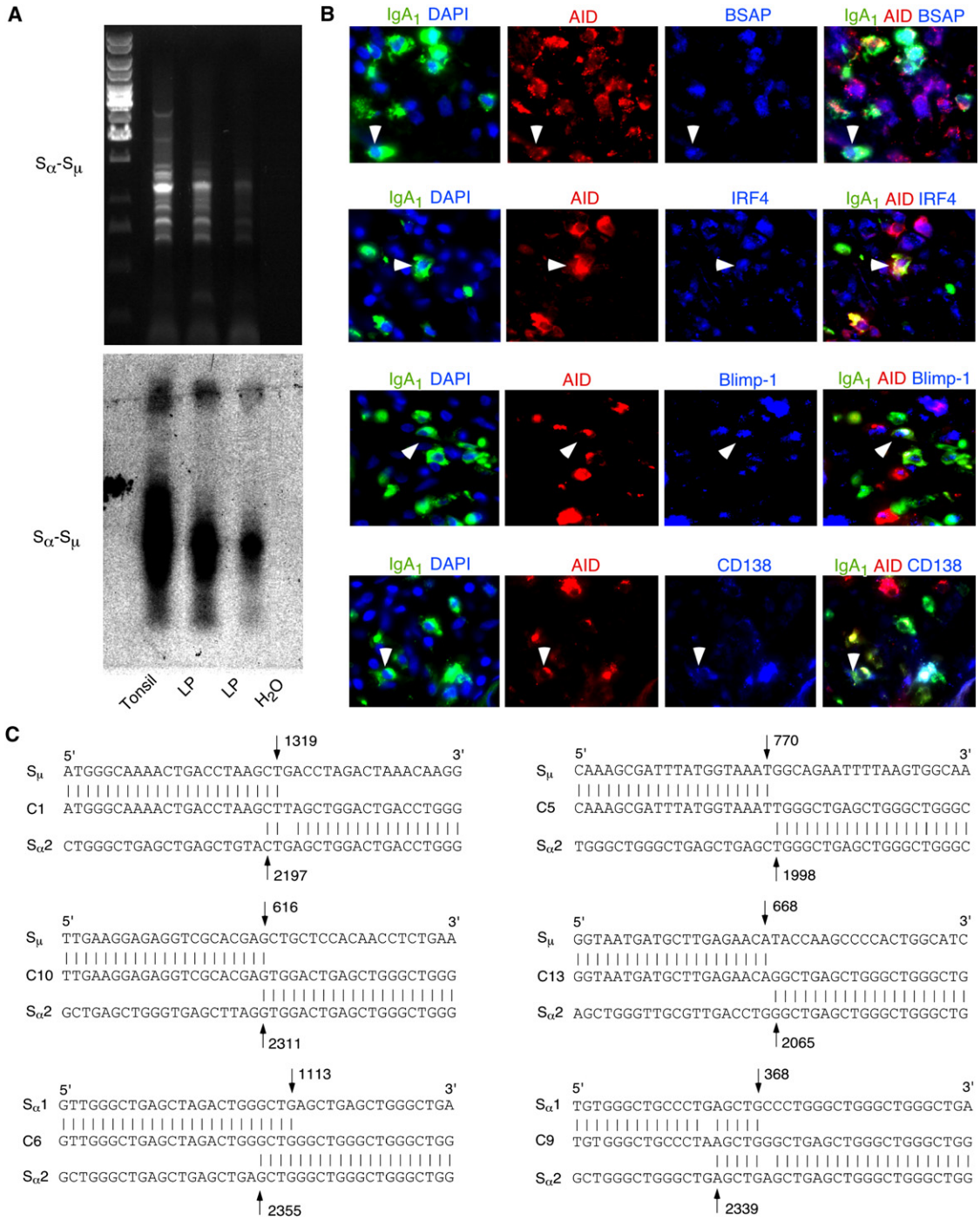

Figure 5. Intestinal LP B Cells Actively Undergo IgA CSR

(A) Extrachromosomal S_α-S_μ switch circles PCR amplified from tonsillar or colon LP B cells (top) and Southern hybridized with an appropriate S_μ probe (bottom). Leftmost and rightmost lanes contain a 1 Kb DNA marker and no genomic DNA, respectively.

(B) Immunofluorescence analysis of intestinal LP stained for IgA_1 (green), AID (red), and BSAP, IRF4, Blimp-1, CD138, and/or DAPI (blue). Arrowheads point to $IgA_1^+AID^+$ LP B cells expressing a transitional GC-plasmacytoid phenotype. Original magnification, ×63.

(C) Sequences of chromosomal S_μ-$S_\alpha2$ and S_μ-$S_\alpha1$-$S_\alpha2$ junctions from LP IgA_2^+ B cells obtained after intestinal tissue digestion. The S_μ portion of S_μ-$S_\alpha1$-$S_\alpha2$ junctions is not shown for clarity. Dashes indicate identities. Arrows indicate the breakpoint site within the S_μ, $S_\alpha1$, or $S_\alpha2$ region (top and bottom sequences) as given in the EMBL/GenBank/DDBJ database.

Shown in (A) and (B) are 1 of 3 experiments yielding similar results.

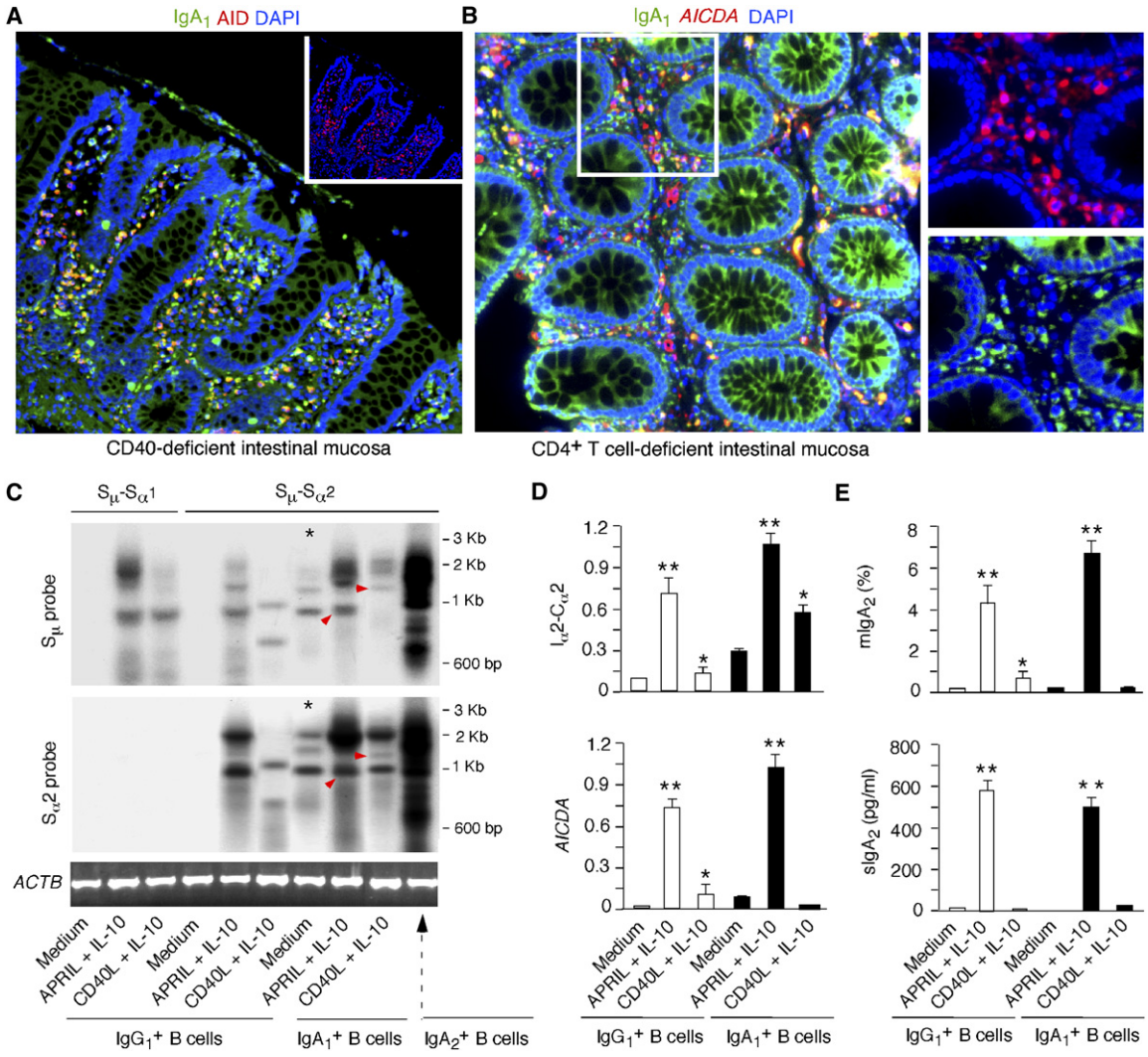

Figure 6. Intestinal LP B Cells Undergo IgA_2 CSR without Help from $CD4^+$ T Cells or CD40L

(A) Immunofluorescence analysis of intestinal mucosa from a CD40-deficient HIGM3 patient stained for IgA_1 (green), AID (red), and DAPI (blue). Upper right inset shows AID and DAPI only. Original magnification, ×40.

(B) Immunofluorescence analysis and in situ hybridization of intestinal mucosa from a $CD4^+$ T cell-deficient AIDS patient stained for IgA_1 (green), *AICDA* (red), and DAPI (blue). Open box in leftmost image corresponds to magnified *AICDA*$^+$ or IgA_1^+ B cells in rightmost panels. Original magnification, ×10 (left) and ×20 (right).

(C) Chromosomal S_μ-$S_\alpha1$ and S_μ-$S_\alpha2$ junctions were PCR amplified from PB IgG_1^+ or IgA_1^+ B cells incubated with or without IL-10, APRIL, and/or CD40L for 4 days and then Southern hybridized with appropriate radiolabeled S_μ or $S_\alpha2$ probes. In the rightmost lane, S_μ-$S_\alpha2$ DNA junctions from sorted colon IgA_2^+ B cells are a positive control. Genomic *ACTB* is a loading control. Asterisk indicates spontaneous IgA_2 CSR, whereas arrowheads indicate bands subjected to cloning and sequencing.

(D) Real-time RT-PCR of $I_\alpha2$-$C_\alpha2$ and *AICDA* transcripts from PB IgG_1^+ or IgA_1^+ B cells incubated as in (C) for 8 days. $I_\alpha2$-$C_\alpha2$ and *AICDA* mRNAs were normalized to *ACTB* mRNA.

(E) Flow cytometric analysis of $mIgA_2$ and ELISA of $sIgA_2$ from PB IgG_1^+ or IgA_1^+ B cells incubated as in (C) for 4 or 8 days.

Shown in (A)–(C) are 1 of 3 experiments yielding similar results, and (D) and (E) summarize 3 experiments (bars indicate mean SD;*$p < 0.05$,**$p < 0.005$ versus medium alone).

is consistent with the relative rarity of IgG in the intestinal LP (Brandtzaeg et al., 2001). It is tempting to speculate that some IgG^+ B cells colonize the LP to amplify the local IgA_2 repertoire via sequential IgG-to-IgA_2 CSR.

A large fraction of intestinal IgA_2^+ plasmablasts derives from local IgD^+ precursors, because LP B cells contained AID and extrachromosomal S_μ-S_α switch circles, two hallmarks of ongoing IgA CSR, in addition to chromosomal S_μ-$S_{\alpha2}$ DNA junctions. Accordingly, APRIL triggered IgA_2 CSR in IgD^+ B cells. Unlike LP IgA_1^+ and IgG_1^+ B cells, which likely derive from PPs (Brandtzaeg et al., 2001), at least some LP IgD^+ B cells may originate from the circulation and could include marginal zone-like B cells (Suzuki et al., 2005; Weller et al., 2004). In agreement with this

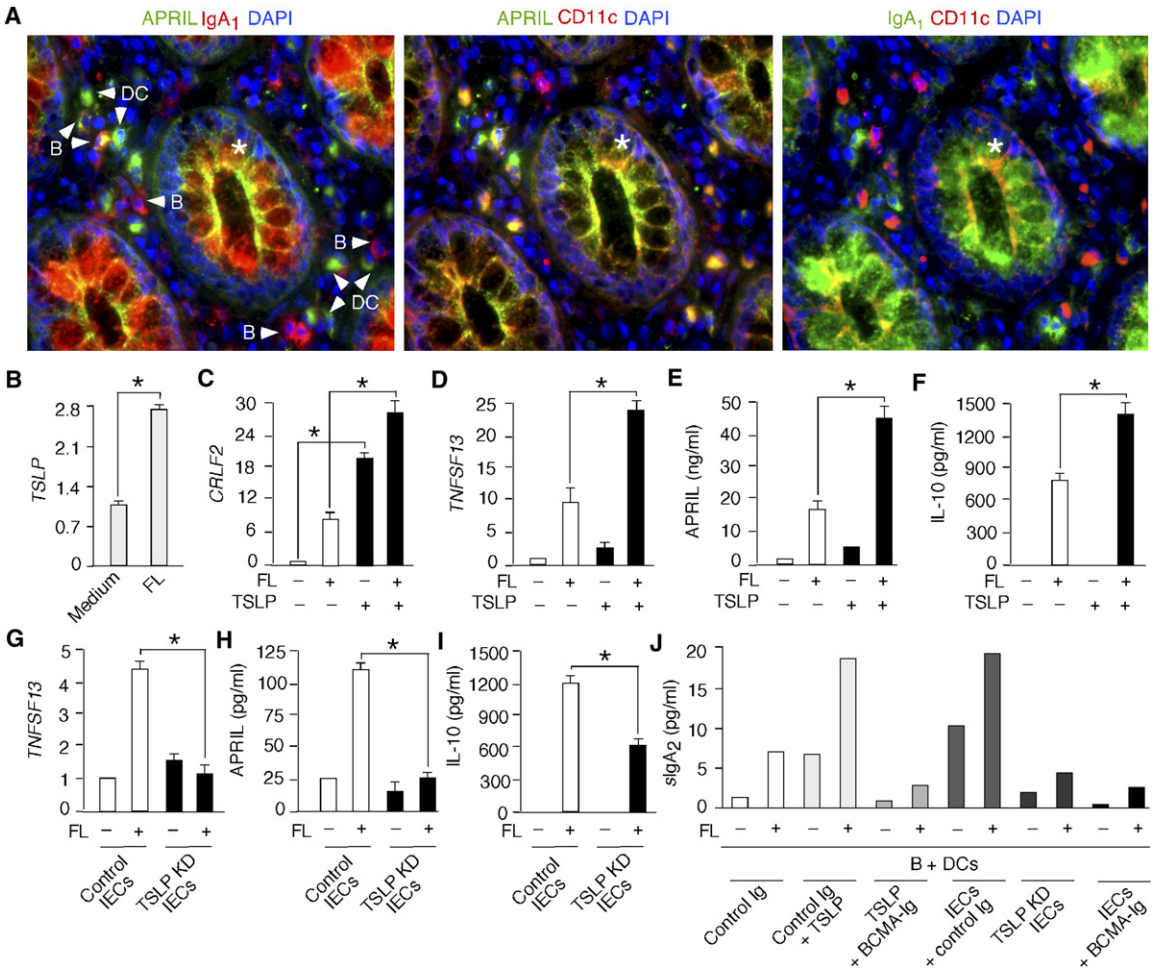

Figure 7. IECs Enhance IgA$_2$ Production by Activating DCs through TSLP

(A) Immunofluorescence analysis of intestinal mucosa stained for APRIL or IgA$_1$ (green), CD11c or IgA$_1$ (red), and DAPI (blue). Asterisk points to an intraepithelial APRIL$^+$IgA$_1^-$CD11c$^+$ DC. Original magnification, ×40.

(B) Real-time RT-PCR of *TSLP* from Caco-2 IECs incubated with or without flagellin (FL) for 2 days. Flagellin was added from the apical surface of IECs, and *TSLP* mRNA was normalized to *ACTB* mRNA.

(C–F) Real-time RT-PCR of *CRLF2* and *TNFSF13* and ELISAs of APRIL and IL-10 from DCs incubated with or without flagellin (FL) and/or TSLP for 2 days. *CRLF2* and *TNFSF13* mRNAs were normalized to *ACTB* mRNA.

(G–I) Real-time RT-PCR of *TNFSF13* and ELISAs of APRIL and IL-10 from DCs incubated with or without flagellin (FL) in the presence or absence of TSLP-sufficient (control) or TSLP-deficient IECs for 2 days.

(J) ELISA of sIgA$_2$ from PB IgD$^+$ B cells exposed to DCs with or without flagellin (FL), TSLP, control Ig, and/or BCMA-Ig in the presence or absence of TSLP-sufficient or TSLP-deficient Caco-2 IECs for 8 days.

Shown in (A) is 1 of 3 experiments yielding similar results, and (B)–(J) summarize 3 experiments (bars indicate mean SD;*$p < 0.05$).

possibility, some mucosal IgA$_2$ reacts against TI antigens, including bacterial polysaccharides, the same way IgM from marginal zone-like B cells does (Mestecky et al., 1999; Weller et al., 2004).

When exposed to recombinant or IEC-derived APRIL, a subset of IgD$^+$ B cells produced IgA$_2$ antibodies naturally reactive against commensal bacteria and their products, including LPS. This production required additional signals from flagellin, a TLR5 ligand, suggesting that TLRs may be critical to link LP IgD$^+$ B cells with the intestinal microflora. Similar to mouse B-1 cells (Fagarasan et al., 2001), human polyreactive IgD$^+$ B cells would enforce IgA$_2$-mediated exclusion of lumenal bacteria by undergoing TI IgA$_2$ CSR in the LP. Accordingly, the intestinal LP of patients lacking CD4$^+$ T cells, CD40, and/or GCs expressed as much IgA$_2$ and AID as the intestinal LP of healthy subjects. Two TI IgA$_2$-inducing pathways would be at work in the human LP. The first involves release of APRIL by IECs as a result of TLR signals generated by commensals, whereas the second implicates APRIL and IL-10 production by mucosal DCs receiving conditioning signals from IEC-derived TSLP.

Together with prior studies (Litinskiy et al., 2002; Macpherson and Uhr, 2004; Rescigno et al., 2001), our data

suggest that intestinal DCs acquire B cell-licensing functions after sampling bacteria from the lumen. In particular, DCs produce IgA_2 CSR-inducing factors, such as APRIL and IL-10, after receiving instructing signals from bacteria and IECs via TLR ligands and TSLP, respectively. Overall, our data indicate that intestinal bacteria trigger IgA_2 class switching via a TI pathway linking IECs with DCs and B cells through an APRIL-mediated TLR-dependent signaling program. Thus, mucosal vaccines should activate IECs to stimulate more effective production of protease-resistant IgA_2 antibodies.

EXPERIMENTAL PROCEDURES

B Cells

PB and tonsillar B cells were purified as reported (Cerutti et al., 2002; Litinskiy et al., 2002; Xu et al., 2007). PB IgD^+, PB IgG_1^+, PB IgA_1^+, and tonsillar IgA_2^+ B cells were magnetically sorted with biotinylated mouse mAbs 2032-08 to IgD, 4E3 to IgG_1, B3506B4 IgA_1, and A9604D2 to IgA_2 (Southern Biotec), respectively, and anti-biotin MicroBeads (Miltenyi Biotec). Purity after sorting was consistently $\geq$97%. LP $CD19^+$ and $IgA2^+$ B cells were purified from LP mononuclear cells obtained upon enzymatic digestion of nonneoplastic specimens of patients undergoing resection for colon carcinoma (distance from the neoplasm >8 cm) as described in the Supplemental Experimental Procedures. LP $CD19^+$ B cells ranged from 6 to 15 × 10^6, whereas LP IgA_2^+ B cells ranged from 4 to 6 × 10^6. Both cell types were >95% pure. The Institutional Review Board of Weill Medical College of Cornell University approved studies with tonsillar and LP cells, and patients provided informed consent. The cell line Ramos was used as a positive control for *AICDA* expression.

DCs

Myeloid dendritic cells were obtained from PB monocytes. In brief, monocytes were sorted with a biotinylated mAb to CD14 (Serotec) and streptavidin MicroBeads and then cultured for 6–8 days in medium RPMI 1640 (Invitrogen) supplemented with 5% human AB serum (Sigma), 1000 U/ml of granulocyte monocyte-colony stimulating factor (Berlex Laboratories), and 1000 U/ml of IL-4 (R&D Systems). Every 2 days, 400 μl of medium was removed from each well and replaced by 500 μl of fresh medium with cytokines. After 6 days, more than 95% of the cells in culture expressed DC-specific antigens, including CD11c, CD40, CD83, CD86, HLA-II, DEC-205, mannose receptor, and DC-specific intercellular adhesion molecule-3 grabbing nonintegrin (DC-SIGN), but less than 10% expressed CD14.

IECs and Other Epithelial Cells

HT-29, Caco-2, T84, and HCA7 IEC lines were derived from human colon carcinoma. All functional assays involving IECs were performed with Caco-2 IECs, which recapitulate most of the properties of primary human IECs, including formation of a polarized monolayer connected by tight junctions (Rescigno et al., 2001; Rimoldi et al., 2005). Lung A549, uterine RL95-2, kidney 293, and cervical HeLa epithelial cell lines as well as primary epidermal (Cambrex Bio Science Walkersville) and oral (MatTek Corporation) epithelial cells were used for control studies. HT-29, Caco-2, T84, HCA7, A549, RL95-2, 293, and HeLa epithelial cell lines were cultured in RPMI 1640 medium or Dulbecco's Modified Eagle's Medium supplemented with 10% fetal calf serum. Primary epidermal and oral ECs were cultured as reported (Xu et al., 2007).

Coculture Systems

Caco-2 IECs were cultured in the upper chamber of 3.0 μm pore Transwell filters (BD PharMingen) for 7 days in a 24-well plate until a transepithelial resistance of ~300 Ω/cm^2 was achieved. B cells (1.0 × 10^6) and DCs (0.2 × 10^6) were seeded in the lower chamber. Filters were treated with bacteria (10 bacteria to 1 IEC) or bacterial products from the apical surface. At 1 hr after incubation, bacteria were washed out and the medium was replaced with medium containing 100 μg/ml of gentamycin. Cocultures were carried out in complete RPMI 1640 medium supplemented with 10% bovine serum.

Bacterial Strains and Products

The following *Salmonella typhimurium* strains on SL1344 background were provided by G. Dougan (Imperial College, London, UK): metabolically defective invasive strain (*aroA*), with attenuated ability to replicate in vivo in mice, and metabolically defective noninvasive strain (*aroA-invA* mutant), defective in the *invA* gene and therefore unable to form productive type-three secretion system. These strains were grown with appropriate antibiotics to preserve carried mutations. *Lactobacillus plantarum* NCIMB882 was grown at 37°C without agitation in MRS broth (Biokar Diagnostic). The *Bacillus subtilis* 168-derivative JH642 was obtained from the *Bacillus* Genetic Stock Center (Columbus, Ohio) and grown at 37°C in 2X YT medium (GIBCO-BRL). Poly(I:C), PGN from *Escherichia coli* 0111:B4 (InvivoGen), flagellin from *Bacillus subtilis*, LPS from *Escherichia coli* 0111:B4 (Sigma), and CpG ODN (Operon Technologies) were used at 20 μg/ml, 20 μg/ml, 0.5 μg/ml, 20 μg/ml, and 20 μg/ml, respectively.

Other Reagents

APRIL (R&D Systems), BAFF (Alexis), CD40L (Immunex), IL-10 (Schering-Plough), and TSLP (R&D Systems) were used at 500 ng/ml, 500 ng/ml, 200 ng/ml, 50 ng/ml, and 30 ng/ml, respectively. APRIL was blocked with 5 μg/ml of BCMA-Ig (Ancell). Mouse MOPC21 IgG_1 with irrelevant binding activity was used at 5 μg/ml to control BCMA-Ig. In IgD^+ B cell cultures, an H15100 polyclonal antibody (pAb) to the μ chain of Igs (Caltag Laboratories) was added at 2 μg/ml to optimize IgA secretion.

Flow Cytometry

The following fluorescein (FITC)-, phycoerythrin or allophycocyanin-conjugated mAbs were used: IADB6 to IgD, SA-DA4 to IgM, A9604D2 to IgA, H2 to IgG, B3506B4 to IgA_1, A9604D2 to IgA_2 (Southern Biotech), and F3637 to IgE (Sigma-Aldrich). At least 1 × 10^4 viable cells were acquired with a FACScalibur analyzer (BD PharMingen).

Enzyme-Linked Immunoadsorbent Assays

ELISAs for total IgA antibodies and IL-10 were described previously (Xu et al., 2007). To measure IgA_1 and IgA_2, Immulon 4 HBX microplates (Thermo Electron Corp.) were coated with a goat $F(ab')_2$ polyclonal antibody (pAb) to human Igs (Cappel) and with a mouse mAb 14A to human IgA_2 (Serotec), respectively, in carbonate-bicarbonate buffer. Then, a biotin-labeled mouse mAb B3506B4 to human IgA_1 or a biotin-labeled mouse A9604D2 mAb to human IgA_2 (Southern Biotech) were added followed by peroxidase-conjugated streptavidin (Vector Laboratories) and TMB Microwell Peroxidase Substrate Kit (Kirkegaard and Perry). Readings were done at 450 nm. A similar strategy was employed to measure IgA_2 to LPS and flagellin, except that microplates were coated with 20 μg/ml of LPS (Sigma) and 10 μg/ml of flagellin (Sigma), respectively. IgA_2 to *Lactobacillus plantarum* were measured by coating microplates with mAb 14A and by sequentially adding bacteria and mAb A9604D2. To measure APRIL, microplates were reacted with a rabbit ED2 mAb (ProSci Inc.) and a biotin-labeled goat BAF884 pAb (R&D Systems).

Immunofluorescence and Immunohistochemistry

Caco-2 IECs stained with an unconjugated rabbit pAb ED2 to APRIL (Pro Sci) and an appropriate secondary reagent were analyzed by immunofluorescence as reported (Litinskiy et al., 2002). Intestinal tissue samples were obtained from five non-AIDS patients and one AIDS patient undergoing resection for colon carcinoma (distance from the neoplasm was more than 8 cm). The PB $CD4^+$ T cell count of the AIDS patient was 2 cells/ml. Additional intestinal tissue sections were obtained from a HIGM3 patient carrying a mutated *CD40* gene. The immunological and molecular features of this case, which corresponds to "Patient 1"

described in a recent report (Ferrari et al., 2001), are summarized in the Supplemental Experimental Procedures. The Institutional Review Board of Weill Medical College of Cornell University approved the study and patients provided informed consent. Tissue sections 5 μm in thickness were paraformaldehyde fixed and then stained with the following primary antibodies: biotin-conjugated mouse mAbs $F(ab')_2$ B3506B4 to IgA_1, $F(ab')_2$ A9604D2 to IgA_2 (Southern Biotech), 1D6 to BAFF (eBioscience), and 3.9 to CD11c (Ancell); goat $F(ab')_2$ pAbs 2032-02 to IgD, 2042-08 to IgG (Southern Biotech), and sc-6059 to IRF4 (Santa Cruz); unconjugated mouse mAbs A-11 to BSAP (Santa Cruz), PG-B6p to Bcl6 (Dako), 3H2-E8 to Blimp-1 (Novus Biologicals), and RPA-T4 to CD4 (Research Diagnostic, Inc.); unconjugated rabbit pAbs H-240 to pan-cytokeratin (Santa Cruz) and ED2 to APRIL (Pro Sci); unconjugated rat mAb EK2-5G9 to AID (Ascenion GmbH, Germany); and, finally, FITC-conjugated mouse mAb 85B152.5 to TLR5 (Imgenex). Control primary antibodies included FITC-conjugated, biotin-conjugated, or unconjugated mouse IgG_1 mAbs, unconjugated rat IgG2a mAb, biotin-conjugated goat $F(ab')_2$ pAb, and unconjugated rabbit pAb. Slides were incubated with the following secondary reagents: indodicarbocyanine-conjugated anti-mouse pAb, rhodamine-conjugated anti-mouse pAb (Jackson ImmunoResearch Laboratories), Alexa Fluor 546/488-conjugated anti-goat pAb, Alexa Fluor 647-conjugated anti-rabbit pAb, and cyanine 3/5-conjugated or rhodamine-conjugated streptavidin (Molecular Probes). Nuclei were visualized with DAPI, 4',6-diamidine-2′-phenylindole dihydrochloride (Boehringer Mannheim). Images were acquired with an Axiovert 200M microscope (Carl Zeiss).

In Situ RNA Hybridization

Full-length *AICDA* cDNA under the control of the SP6 promoter was used as template to transcribe an antisense RNA probe with a commercial riboprobe generation kit containing biotin-labeled UTP (Roche Applied Science) as previously reported (Xu et al., 2007). A sense RNA probe was used as negative control. Tissue sections were fixed, hybridized, and stained as described in the Supplemental Experimental Procedures.

Conventional and Quantitative Real-Time RT-PCRs

TNFSF13, *AICDA*, and *ACTB* transcripts were RT-PCR amplified as reported (Litinskiy et al., 2002). MYD88, I_μ-$C_\alpha1$, and I_μ-$C_\alpha2$ were RT-PCR amplified with MYD88 forward 5′-GAGCGTTTCGATGCCTTCAT-3′ plus MYD88 reverse 5′-CGGATCATCTCCTGCACAAA-3′ and I_μ forward 5′-GTGATTAAGGAGAAACACTTTGAT-3′ plus either $C_\alpha1$ reverse 5′-GGGTGGCGGTTAGCGGGGTCTTGG-3′ or $C_\alpha2$ reverse 5′-TGTTGGCGGTTAGTGGGGTCTTGCA-3′. *AICDA*, I_α-C_μ, I_μ-C_μ, *TSLP*, *CRFL2*, and *ACTB* were quantitated through real-time RT-PCR as described (Xu et al., 2007). $I_\alpha2$-$C_\alpha2$ and *TNFSF13* were quantitated with $I_\alpha2$-$C_\alpha2$ forward 5′-CTCAGCACTGCGGGCCCTCCA-3′ plus $I_\alpha2$-$C_\alpha2$ reverse 5′-GTTCCCATCTTGGGGGGTGCTGTC-3′ and with *TNFSF13* forward 5′-GTGATGTGGCAACCAGCTCTT-3′ plus *TNFSF13* reverse 5′-CCCTTGGTGTAAATGGAAGAC-3′, respectively.

Microdissection

Intestinal specimens were frozen in Tissue-Tek optimum cutting temperature compound (Sakura). Cryostat sections were affixed to glass foil slides for membrane-based laser microdissection (Leica), allowed to dry for 30 min at 20°C–25°C, fixed for 1 min in 70% ethanol, washed for 30 s in distilled water, stained for 1 min with 0.6% (weight/volume) methyl green (Fluka), rinsed in distilled water, dehydrated by a graded ethanol series (70%, 95%, and 100%) for 1 min each, and allowed to air dry at 20°C–25°C for 7–12 hr. LP regions containing at least 200 IgA^+ B cells were isolated by laser-capture microdissection on a Leica AS LMD and collected in a 2 ml microcentrifuge tube for DNA extraction and amplification.

Genomic DNA PCR and Southern Blots

Genomic DNA was extracted from B cells with miniDNA preparation kit (Qiagen) and from microdissected LP specimens with QIAamp DNA micro kit (Qiagen). Chromosomal S_μ-$S_\alpha1$ and S_μ-$S_\alpha2$ junctions were amplified with an S_μ forward primer 5′-CTTGTTAATGGACTTGGAG GAATGATTCC-3′ and either a $S_\alpha1$ reverse primer 5′-ACTGTGAGG ACGCGGCCCTCTCCT-3′ or a $S_\alpha2$ reverse primer 5′-AATGCGCTGT GAGGACGCGGCCCTCATGC-3′. Elongase (Invitrogen) was used under the following conditions: denaturation 1 min at 94°C, annealing 2 min at 62°C, and extension 3 min at 72°C for 30 cycles. A second PCR was performed on the DNA product of the first PCR under similar conditions, but with the nested S_μ forward primer 5′-GCTGCTG CATTTGCTTCTCTTAAAAC-3′ and the nested $S_\alpha2$ reverse primer 5′-AGCCCACCCCAGGGCAGCTCAGTAC-3′. To verify their identity to S_μ-$S_\alpha2$ junctions, PCR amplicons were fractionated onto a 0.8% agarose gel, transferred overnight onto nylon membranes, and hybridized with a radiolabeled probe spanning residues 274–497 of the 5′ portion of S_μ. Then, membranes were stripped and hybridized with a radiolabeled probe spanning residues 3199–3238 of the 3′ portion of $S_\alpha2$. Extrachromosomal S_α-S_μ junctions were PCR amplified as reported (Litinskiy et al., 2002) and hybridized with a radiolabeled probe recognizing the 3′ portion of S_μ as described in the Supplemental Experimental Procedures. Genomic *ACTB* and I_μ-C_μ transcripts were detected as reported (Litinskiy et al., 2002). I_μ-$C_\alpha1$ and I_μ-$C_\alpha2$ transcripts were hybridized with a radiolabeled consensus C_α 5′-CGAC ACGGGTCGGTACCTTGGTACCC-3′ oligoprobe.

Cloning and Sequencing

0.5–3 Kb PCR products hybridizing with both S_μ and $S_\alpha2$ probes were gel purified (Qiagen) and cloned into a PCR2.1 TOPO vector with a TA cloning kit (Invitrogen). Positive clones were PCR identified with the S_μ forward primer 5′-CCACTAGAAGGGGAACTGGTCTTA-3′ and the $S_\alpha2$ reverse primer 5′-AGCCCACCCCAGGGCAGCTCAGTAC-3′. The percentage of positive clones ranged from 90% to 94%. Positive clones were purified and sequenced as described in the Supplemental Experimental Procedures.

RNA Interference and Nucleofection

TSLP-deficient Caco-2 IECs were generated as described (Rimoldi et al., 2005). To knock down MYD88, a psiRNA-hMyD88 plasmid expressing a MYD88-targeting small interfering RNA (siRNA) or a plasmid expressing control siRNA (Invivogen) was resuspended with 1.0×10^6 IECs into 100 μl of human keratinocyte nucleofector solution (Amaxa). Plasmids were nucleofected with an appropriate device (Amaxa). To knock down *TNFSF13*, 0.4 μl of a 20 μM Hs_ATGGCTCTGCTGACCC AACAA_1_HP APRIL siRNA or control siRNA (Qiagen) were incubated with 6 μl of HiPerFect Transfection Reagent (Qiagen) in 200 μl of serum-free DMEM medium for 5–10 min at room temperature. This mixture was added drop-wise to 3×10^5 EC cells, which were then incubated at 37°C. Expression of targeted mRNA and proteins was evaluated after 24 and 48 hr, respectively.

Western Blot

Protein extracts were transferred to nylon membranes as reported (Xu et al., 2007). After blocking, membranes were probed with primary goat pAbs to APRIL (R-15), MyD88 (N-19), or actin (I-19) (Santa Cruz Biotechnologies). Membranes were washed and incubated with an appropriate secondary antibody (Santa Cruz). Proteins were detected with an enhanced chemiluminescence detection system (Amersham).

Statistical Analysis

For immunoglobulin secretion, proliferation, survival, and reporter assays, values were calculated as mean standard deviation for at least three separate experiments done in triplicate. The significance of differences between experimental variables was determined with the Student's t test.

Supplemental Data

Twelve figures and Experimental Procedures are available at http://www.immunity.com/cgi/content/full/26/6/812/DC1/.

ACKNOWLEDGMENTS

We thank M. Rimoldi (European Institute of Oncology, Milan, Italy) for preparing Caco-2 cells and bacteria and A. Dannenberg (Weill Medical College of Cornell University, New York, NY) for generating dendritic cells and providing HT-29 cells. This work was supported by NIH grant AI057653 (to A. Cerutti), funds from NIH T32 grant AI07621 (to W.X.), and funds from Fondazione C. Golgi and Centro Immunodeficienze Mario Di Martino (A.P.). B.H. and W.X. equally contributed to this work by performing research and analyzing and discussing data; P.A.S., J.E., and M.S. performed research; A. Chiu, A. Chadburn, A.D.P., C.R.R., V.V., A.P., and D.M.K. provided tissue samples and discussed data; M.R. provided essential reagents, discussed data, and critically read the paper; and A. Cerutti designed research, analyzed data, and wrote the paper.

Received: December 10, 2006
Revised: April 2, 2007
Accepted: April 25, 2007
Published online: June 14, 2007

REFERENCES

Abreu, M.T., Fukata, M., and Arditi, M. (2005). TLR signaling in the gut in health and disease. J. Immunol. *174*, 4453–4460.

Brandtzaeg, P., Baekkevold, E.S., and Morton, H.C. (2001). From B to A the mucosal way. Nat. Immunol. *2*, 1093–1094.

Calame, K.L. (2001). Plasma cells: finding new light at the end of B cell development. Nat. Immunol. *2*, 1103–1108.

Castigli, E., Alt, F.W., Davidson, L., Bottaro, A., Mizoguchi, E., Bhan, A.K., and Geha, R.S. (1994). CD40-deficient mice generated by recombination-activating gene-2-deficient blastocyst complementation. Proc. Natl. Acad. Sci. USA *91*, 12135–12139.

Castigli, E., Scott, S., Dedeoglu, F., Bryce, P., Jabara, H., Bhan, A.K., Mizoguchi, E., and Geha, R.S. (2004). Impaired IgA class switching in APRIL-deficient mice. Proc. Natl. Acad. Sci. USA *101*, 3903–3908.

Castigli, E., Wilson, S.A., Scott, S., Dedeoglu, F., Xu, S., Lam, K.P., Bram, R.J., Jabara, H., and Geha, R.S. (2005). TACI and BAFF-R mediate isotype switching in B cells. J. Exp. Med. *201*, 35–39.

Cattoretti, G., Buttner, M., Shaknovich, R., Kremmer, E., Alobeid, B., and Niedobitek, G. (2006). Nuclear and cytoplasmic AID in extrafollicular and germinal center B cells. Blood *107*, 3967–3975.

Cerutti, A., Zan, H., Kim, E.C., Shah, S., Schattner, E.J., Schaffer, A., and Casali, P. (2002). Ongoing in vivo immunoglobulin class switch DNA recombination in chronic lymphocytic leukemia B cells. J. Immunol. *169*, 6594–6603.

Chaudhuri, J., and Alt, F.W. (2004). Class-switch recombination: interplay of transcription, DNA deamination and DNA repair. Nat. Rev. Immunol. *4*, 541–552.

Coffman, R.L., Lebman, D.A., and Shrader, B. (1989). Transforming growth factor beta specifically enhances IgA production by lipopolysaccharide-stimulated murine B lymphocytes. J. Exp. Med. *170*, 1039–1044.

Crago, S.S., Kutteh, W.H., Moro, I., Allansmith, M.R., Radl, J., Haaijman, J.J., and Mestecky, J. (1984). Distribution of IgA1-, IgA2-, and J chain-containing cells in human tissues. J. Immunol. *132*, 16–28.

Fagarasan, S., and Honjo, T. (2003). Intestinal IgA synthesis: regulation of front-line body defences. Nat. Rev. Immunol. *3*, 63–72.

Fagarasan, S., Kinoshita, K., Muramatsu, M., Ikuta, K., and Honjo, T. (2001). In situ class switching and differentiation to IgA-producing cells in the gut lamina propria. Nature *413*, 639–643.

Fagarasan, S., Muramatsu, M., Suzuki, K., Nagaoka, H., Hiai, H., and Honjo, T. (2002). Critical roles of activation-induced cytidine deaminase in the homeostasis of gut flora. Science *298*, 1424–1427.

Fayette, J., Dubois, B., Vandenabeele, S., Bridon, J.M., Vanbervliet, B., Durand, I., Banchereau, J., Caux, C., and Briere, F. (1997). Human dendritic cells skew isotype switching of CD40-activated naive B cells towards IgA1 and IgA2. J. Exp. Med. *185*, 1909–1918.

Ferrari, S., Giliani, S., Insalaco, A., Al-Ghonaium, A., Soresina, A.R., Loubser, M., Avanzini, M.A., Marconi, M., Badolato, R., Ugazio, A.G., et al. (2001). Mutations of CD40 gene cause an autosomal recessive form of immunodeficiency with hyper IgM. Proc. Natl. Acad. Sci. USA *98*, 12614–12619.

He, B., Qiao, X., and Cerutti, A. (2004). CpG DNA induces IgG class switch DNA recombination by activating human B cells through an innate pathway that requires TLR9 and cooperates with IL-10. J. Immunol. *173*, 4479–4491.

Hel, Z., McGhee, J.R., and Mestecky, J. (2006). HIV infection: first battle decides the war. Trends Immunol. *27*, 274–281.

Honjo, T., Kinoshita, K., and Muramatsu, M. (2002). Molecular mechanism of class switch recombination: linkage with somatic hypermutation. Annu. Rev. Immunol. *20*, 165–196.

Jain, A., Ma, C.A., Lopez-Granados, E., Means, G., Brady, W., Orange, J.S., Liu, S., Holland, S., and Derry, J.M. (2004). Specific NEMO mutations impair CD40-mediated c-Rel activation and B cell terminal differentiation. J. Clin. Invest. *114*, 1593–1602.

Kato, A., Truong-Tran, A.Q., Scott, A.L., Matsumoto, K., and Schleimer, R.P. (2006). Airway epithelial cells produce B cell-activating factor of TNF family by an IFN-beta-dependent mechanism. J. Immunol. *177*, 7164–7172.

Kett, K., Brandtzaeg, P., Radl, J., and Haaijman, J.J. (1986). Different subclass distribution of IgA-producing cells in human lymphoid organs and various secretory tissues. J. Immunol. *136*, 3631–3635.

Klein, U., Casola, S., Cattoretti, G., Shen, Q., Lia, M., Mo, T., Ludwig, T., Rajewsky, K., and Dalla-Favera, R. (2006). Transcription factor IRF4 controls plasma cell differentiation and class-switch recombination. Nat. Immunol. *7*, 773–782.

Litinskiy, M.B., Nardelli, B., Hilbert, D.M., He, B., Schaffer, A., Casali, P., and Cerutti, A. (2002). DCs induce CD40-independent immunoglobulin class switching through BLyS and APRIL. Nat. Immunol. *3*, 822–829.

Lue, C., Tarkowski, A., and Mestecky, J. (1988). Systemic immunization with pneumococcal polysaccharide vaccine induces a predominant IgA2 response of peripheral blood lymphocytes and increases of both serum and secretory anti-pneumococcal antibodies. J. Immunol. *140*, 3793–3800.

Macpherson, A.J. (2006). IgA adaptation to the presence of commensal bacteria in the intestine. Curr. Top. Microbiol. Immunol. *308*, 117–136.

Macpherson, A.J., and Uhr, T. (2004). Induction of protective IgA by intestinal dendritic cells carrying commensal bacteria. Science *303*, 1662–1665.

Mestecky, J., Russell, M.W., and Elson, C.O. (1999). Intestinal IgA: novel views on its function in the defence of the largest mucosal surface. Gut *44*, 2–5.

Mora, J.R., Iwata, M., Eksteen, B., Song, S.Y., Junt, T., Senman, B., Otipoby, K.L., Yokota, A., Takeuchi, H., Ricciardi-Castagnoli, P., et al. (2006). Generation of gut-homing IgA-secreting B cells by intestinal dendritic cells. Science *314*, 1157–1160.

Nagler-Anderson, C. (2001). Man the barrier! Strategic defences in the intestinal mucosa. Nat. Rev. Immunol. *1*, 59–67.

Neutra, M.R., Mantis, N.J., and Kraehenbuhl, J.P. (2001). Collaboration of epithelial cells with organized mucosal lymphoid tissues. Nat. Immunol. *2*, 1004–1009.

Odegard, V.H., and Schatz, D.G. (2006). Targeting of somatic hypermutation. Nat. Rev. Immunol. *6*, 573–583.

Rakoff-Nahoum, S., Paglino, J., Eslami-Varzaneh, F., Edberg, S., and Medzhitov, R. (2004). Recognition of commensal microflora by toll-like receptors is required for intestinal homeostasis. Cell *118*, 229–241.

Rescigno, M., Urbano, M., Valzasina, B., Francolini, M., Rotta, G., Bonasio, R., Granucci, F., Kraehenbuhl, J.P., and Ricciardi-Castagnoli, P. (2001). Dendritic cells express tight junction proteins and penetrate gut epithelial monolayers to sample bacteria. Nat. Immunol. *2*, 361–367.

Rimoldi, M., Chieppa, M., Salucci, V., Avogadri, F., Sonzogni, A., Sampietro, G.M., Nespoli, A., Viale, G., Allavena, P., and Rescigno, M. (2005). Intestinal immune homeostasis is regulated by the crosstalk between epithelial cells and dendritic cells. Nat. Immunol. *6*, 507–514.

Salzer, U., Chapel, H.M., Webster, A.D., Pan-Hammarstrom, Q., Schmitt-Graeff, A., Schlesier, M., Peter, H.H., Rockstroh, J.K., Schneider, P., Schaffer, A.A., et al. (2005). Mutations in TNFRSF13B encoding TACI are associated with common variable immunodeficiency in humans. Nat. Genet. *37*, 820–828.

Sato, A., Hashiguchi, M., Toda, E., Iwasaki, A., Hachimura, S., and Kaminogawa, S. (2003). CD11b+ Peyer's patch dendritic cells secrete IL-6 and induce IgA secretion from naive B cells. J. Immunol. *171*, 3684–3690.

Schlissel, M.S. (2003). Regulating antigen-receptor gene assembly. Nat. Rev. Immunol. *3*, 890–899.

Schneider, P. (2005). The role of APRIL and BAFF in lymphocyte activation. Curr. Opin. Immunol. *17*, 282–289.

Stavnezer, J. (1996). Antibody class switching. Adv. Immunol. *61*, 79–146.

Suzuki, K., Meek, B., Doi, Y., Honjo, T., and Fagarasan, S. (2005). Two distinctive pathways for recruitment of naive and primed IgM+ B cells to the gut lamina propria. Proc. Natl. Acad. Sci. USA *102*, 2482–2486.

Takeda, K., Kaisho, T., and Akira, S. (2003). Toll-like receptors. Annu. Rev. Immunol. *21*, 335–376.

Tarkowski, A., Lue, C., Moldoveanu, Z., Kiyono, H., McGhee, J.R., and Mestecky, J. (1990). Immunization of humans with polysaccharide vaccines induces systemic, predominantly polymeric IgA2-subclass antibody responses. J. Immunol. *144*, 3770–3778.

Weller, S., Braun, M.C., Tan, B.K., Rosenwald, A., Cordier, C., Conley, M.E., Plebani, A., Kumararatne, D.S., Bonnet, D., Tournilhac, O., et al. (2004). Human blood IgM "memory" B cells are circulating splenic marginal zone B cells harboring a prediversified immunoglobulin repertoire. Blood *104*, 3647–3654.

Wilson, E., and Butcher, E.C. (2004). CCL28 controls immunoglobulin (Ig)A plasma cell accumulation in the lactating mammary gland and IgA antibody transfer to the neonate. J. Exp. Med. *200*, 805–809.

Xu, W., He, B., Chiu, A., Chadburn, A., Shan, M., Buldys, M., Ding, A., Knowles, D.M., Santini, P.A., and Cerutti, A. (2007). Epithelial cells trigger frontline immunoglobulin class switching through a pathway regulated by the inhibitor SLPI. Nat. Immunol. *8*, 294–303.

Ziegler, S.F., and Liu, Y.J. (2006). Thymic stromal lymphopoietin in normal and pathogenic T cell development and function. Nat. Immunol. *7*, 709–714.